

JGR Biogeosciences

RESEARCH ARTICLE

10.1029/2019JG005306

Key Points:

- Significant spatial variations in crown architecture traits are observed across large climate gradients
- Trunk and leaf traits are correlated with precipitation, while crown architecture is correlated with both temperature and precipitation
- Crown shape related architecture traits coordinate with trunk and leaf traits tightly to adapt to changes in environmental conditions

Supporting Information:

- Supporting Information S1

Correspondence to:

Q. Guo, qguo@ibcas.ac.cn

Citation:






Su, Y., Hu, T., Wang, Y., Li, Y., Dai, J., Liu, H., et al (2020). Large-scale geographical variations and climatic controls on crown architecture traits. *Journal of Geophysical Research: Biogeosciences*, 125, e2019JG005306. <https://doi.org/10.1029/2019JG005306>

Received 12 JUN 2019

Accepted 12 FEB 2020

Accepted article online 13 FEB 2020

Large-Scale Geographical Variations and Climatic Controls on Crown Architecture Traits

Yanjun Su^{1,2} , Tianyu Hu^{1,2}, Yongcai Wang³, Yumei Li^{1,2}, Jingyu Dai⁴, Hongyan Liu⁴ , Shichao Jin^{1,2}, Qin Ma⁵ , Jin Wu⁶, Lingli Liu^{1,2} , Jingyun Fang^{1,4}, and Qinghua Guo^{1,2} 

¹State Key Laboratory of Vegetation and Environmental Change, Institute of Botany, Chinese Academy of Sciences, Beijing, China, ²University of Chinese Academy of Sciences, Beijing, China, ³Satellite Environmental Application Center, Ministry of Environmental Protection, Beijing, China, ⁴College of Urban and Environmental Sciences, Peking University, Beijing, China, ⁵Department of Forestry, Mississippi State University, Mississippi State, MS, USA, ⁶School of Biological Sciences, University of Hong Kong, Pokfulam, Hong Kong

Abstract Crown architecture is a critical component for a tree to interact with the ambient environment and to compete with neighbors. However, little is known regarding how climate variability may shape crown architecture traits across large geographical extents and whether crown architecture traits have coordinated variations with trunk and leaf traits to climate gradients. Here we used *Quercus mongolica* trees as an example, used the cutting-edge terrestrial laser scanning technique to accurately characterize their crown architecture traits, and explored their variabilities along with environmental variability across large climate gradients in northern China. Our results showed that there are significant spatial variations in trunk, crown, and leaf traits even for the same genetic group across large environmental gradients. Tree height and leaf size had tight covariations with precipitation ($|R| > 0.8$, $p < 0.01$). We also observed coordinated variations among crown architecture traits related to canopy shape (e.g., primary branch insertion angle, chord length ratio), trunk traits (e.g., tree height), leaf traits (e.g., specific leaf area), and climate variability, highlighting there are likely fundamental evolutionary strategies regulating these covariations. With a projected drier and hotter climate scenario in this region, our results further suggest trees are expected to transit from a “tree shape” to a “shrub shape,” with large ecological and ecophysiological impacts on this region.

Plain Language Summary Trees under different environmental conditions can show vast diversity in crown architectures. Understanding patterns and proximate causes of such diversity is a central question in plant ecology, with important implications for predicting future vegetation dynamics with climate change. Here, we combined the cutting-edge terrestrial laser scanning technology and field measurements to investigate the role of crown architecture in the evolutionary strategy development of *Quercus mongolica* trees in northern China with large climate gradients. Our findings provide new insights on the hypothesis of how crown architecture traits coordinated with trunk and leaf traits to balance the light and water demands of a tree and highlight the significance of long-neglected crown architecture in tree evolutionary strategy, with important implications in future vegetation dynamic prediction studies.

1. Introduction

Crown architecture is composed by an ensemble of attributes related to branch characteristics and branching pattern of a tree, such as the branch bifurcation ratio, branch orientation, branch diameter, and branch chord length (Ceulemans et al., 1990). Crown architecture traits, together with trunk traits (e.g., tree height and diameter at breast height/DBH) and leaf traits (e.g., leaf size and leaf distribution), define a tree (Figure 1). Through determining the display and distribution of leaves, increasing evidences have shown that crown architecture traits play a fundamental role in the light interception process of a tree and therefore influence the subsequent carbon and water fluxes exchanged between the tree and atmosphere (Forrester et al., 2018; Guisasaola et al., 2015; Hallé et al., 1978). The variations in crown architecture traits can reflect the defensive strategies of trees to the climate variability and tree growth competition (Percy et al., 2004; Percy et al., 2005; Poorter et al., 2003; Poorter et al., 2006; Valladares & Pugnaire, 1999). Understanding the underlying processes that mediate the variability in crown architecture traits is thus an essential first

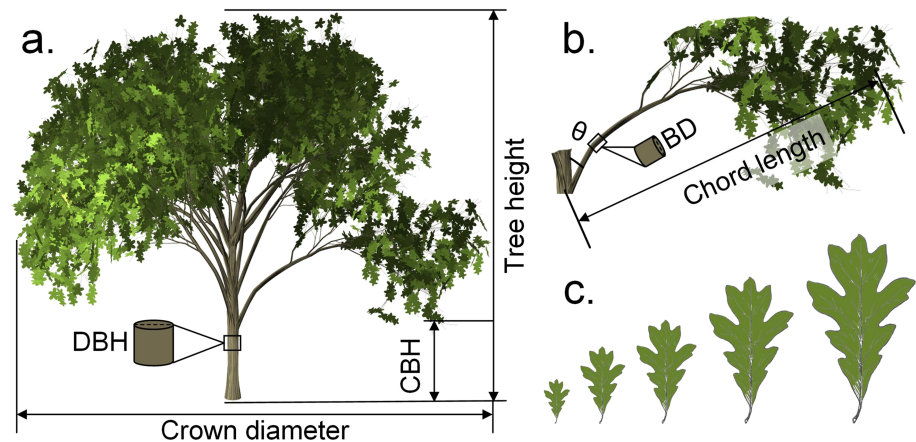


Figure 1. A simulated tree with the demonstration of (a) trunk traits, (b) crown architecture traits, and (c) leaf traits. Note that DBH, CBH, BD, and θ represent diameter at breast height, crown base height, branch diameter, and insertion angle, respectively.

step to help understand the ecological and ecophysiological responses of trees to current and future climate variabilities.

The responses of trunk and leaf traits to the climate variability have been well studied (Fortin et al., 2018; Iida et al., 2011; Niinemets, 2001; Ordoñez et al., 2009; Tingstad et al., 2015; Wright et al., 2017). For example, it was found that taller trees incline to occur at places with higher water availability (Tao et al., 2016) and show higher vulnerability to droughts (Bennett et al., 2015), while at a given latitude of temperate biomes, larger and thinner leaves are easier to be found in a wetter environment (Lusk et al., 2019; Wright et al., 2017). However, crown architecture traits, as an essential link between trunk and leaf traits (Savage et al., 2010), are still much less studied in the fields of ecology and plant physiology (Escudero et al., 2017; Malhi et al., 2018). Although there have been theories predicting that in a light-driven environment, shade-tolerance trees may develop wider crowns and solidier branches, and heliophile trees may have narrower crowns under the canopy and develop larger crowns once reaching open spaces to maximize light capture (Davies & Ashton, 1999; Sterck et al., 2001; Wright et al., 2005), most of these studies are still based on empirical descriptions or model simulations at a local scale (Chave et al., 2005; Escudero et al., 2017; Ishii & Asano, 2010; Malhi et al., 2018; Pearcy et al., 2005; Valladares & Pugnaire, 1999). How crown architecture traits acclimate to the climate variability over large spatial scales and whether there are coordinated relationships among trunk, leaf, and crown architecture traits remain important unknown questions in the field.

One crucial challenge in crown architecture related studies is the lack of efficient and accurate methods to quantify crown architecture traits. Field-based in situ survey is the most commonly used approach, which often involves many highly labor-intensive and time-consuming processes (Bentley et al., 2013), and is thus mainly constrained to small-scale studies. This is particularly true for measuring certain key crown architecture traits (e.g., branch bifurcation ratio, branch chord length ratio, and branch insertion angle), which needs to destructively harvest tree organs. Recent advances in terrestrial laser scanning (TLS) technology are revolutionizing how we look at trees (Dassot et al., 2011; Gonzalez de Tanago et al., 2018). Through the use of a focused short-wavelength laser pulse, TLS has a strong capability to penetrate forest canopy and collect high-fidelity three-dimensional data of trees in the form of point cloud (Calders et al., 2017). Numerous studies have proven that TLS is an objective, accurate, and efficient method to extract trunk traits (e.g., tree height and DBH) (Calders et al., 2015; Li et al., 2017; Liang et al., 2016; Liang et al., 2018; Luo et al., 2018; Vicari et al., 2019; Wang et al., 2019). With the assistance of individual tree segmentation and stem-leaf segmentation algorithms, detailed crown architecture traits are also becoming possible to acquire in a repeatable and accurate way (Disney, 2018; Jin, Su, Gao, et al., 2018; Jin, Su, Wu, et al., 2018; Li et al., 2012; Li et al., 2018; Moorthy et al., 2011; Tao, Guo, et al., 2015; Tao, Wu, et al., 2015), which provides a new tool to observe changes in tree architecture. For example, Jackson et al. (2019) modeled the motion of tree crowns in the wind from TLS data; Puttonen et al. (2016) found that TLS could be used to monitor overnight sleep movements of tree branches and argued that TLS could be used to support chronobiology studies; Magney et al. (2016) proved that TLS could be used to investigate canopy light regime and reveal patterns of

photosynthetic partitioning; Lau et al. (2019) used TLS technique to validate the crown architecture-based metabolic scaling exponents of tropical trees. It is believed that TLS can lead the advances in understanding how tree architectures are influenced by environmental stresses (Malhi et al., 2018).

With the aid of TLS technology, this study aims to address the following three questions. 1) What are geographical distributions of trunk, crown architecture, and leaf traits over large spatial extents? 2) Are there any coordinated variations among trunk, crown architecture, and leaf traits with climate gradients? 3) How does the climate variability mediate the leaf-crown-trunk coordinated relationships? Since crown architecture can show variability with both species diversity and environmental variability (Sterck et al., 2001; Thomas, 1996), we here used *Quercus mongolica*, a rare oak tree species spread in semiarid and semihumid areas of northern China, as an example, but the developed approach can be applied to other tree species. Specifically, we selected 36 plots of 12 study sites (each study site has three plots), covering four *Q. mongolica* genetic groups across northern China. Two trunk traits, nine crown architecture traits, and four leaf traits were acquired from TLS data and field measurements. We aim to link these datasets to help answer the three questions mentioned above.

2. Materials and Methods

2.1. Study Area

Quercus mongolica trees are featured by dramatic variations in crown architecture under different environmental conditions (Kitao et al., 2000; Kitao et al., 2006) (Figures 2b and 2c). The habitats of *Q. mongolica* trees in northern China have four major genetic groups, that is, the northern group, the eastern group, the central group, and the southern group (Figure 2 and supporting information, Table S1). Within each genetic group, three sites were selected using the following rules: 1) each site should be able to find three $\geq 600\text{-m}^2$ rectangular plots dominated by *Q. mongolica* trees and 2) the aspect of the three plots in each site should be as distinct as possible. Finally, 36 plots within 12 sites (populations) across northern China were used to analyze the spatial variations in *Q. mongolica* tree attributes (Figure 2a), which covered an elevation range of 270–2,100 m, a mean annual total precipitation (MAP) range of 330–800 mm, and a mean annual temperature (MAT) range of 1.9–11.6 °C (Table S1).

2.2. TLS Data Acquisition and Preprocessing

A Rigel VZ-400 scanner mounted on a tripod was used to collect TLS data with 10–13 scanning positions for each plot. At each scanning position, one upright scan and one tilted scan (with a tilting angle of 30°) were collected to ensure the completeness of the collected TLS point clouds (Figure 3). Around 15–20 referencing targets with high reflectance were set up in each plot to register the collected TLS data from different scans. At least four referencing targets were made sure that could be visually seen at each scan. The Rigel RiSCAN Pro software was used to register the TLS data from different scans. The final registration errors for all plots were lower than 1 cm.

The registered TLS data of each plot were further processed to remove noise points and generate normalized point clouds to remove terrain effects (Figure 3). In this study, the outlier removal algorithm integrated in the LiDAR360 software was used to reduce noise points in the collected data. This algorithm identifies noise points by determining whether the distance of a point to its surrounding neighbors is larger than $avg. + n \times std.$ (where *avg.* and *std.* are the average and standard deviation of the distances between points and their surrounding neighbors and *n* is a user-defined threshold). Then, we used an improved progressive triangulated irregular network densification filtering algorithm proposed by Zhao et al. (2016) to filter ground points in each TLS dataset. A digital terrain model (DTM) in 10-cm resolution was generated from the ground points using the ordinary kriging method for each plot (Guo et al., 2010). Finally, the TLS data of each plot was normalized by subtracting the DTM value from the original TLS point height at the corresponding location. All processes related to TLS data hereafter were based on normalized TLS data.

2.3. Field Measurements

Beyond TLS acquisitions, we also collected field measurements to derive tree attributes that could not be directly estimated from TLS data (i.e., tree age, leaf area, leaf thickness, leaf vein length, and specific leaf area) (Table 1). Within each plot, all trees with a DBH ≥ 5 cm were first tagged with unique numbers so that they could be recognized from the TLS point clouds, and then their species were recognized and recorded.

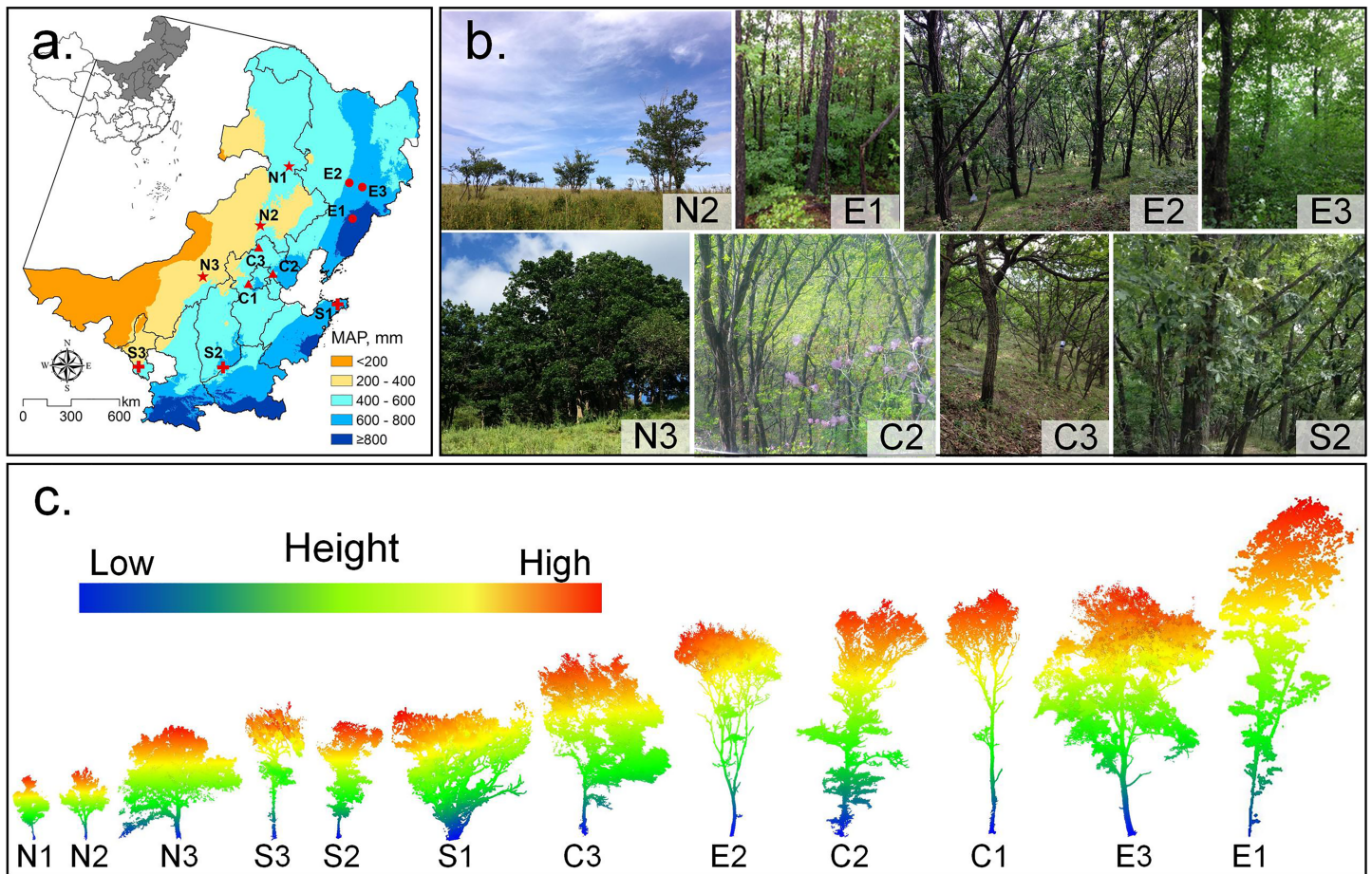


Figure 2. (a) The locations of the 12 study sites and their corresponding mean annual total precipitation (MAP) (the study sites of each genetic group are shown in a unique point shape, and the “N,” “E,” “C,” and “S” in each site ID represent the northern, eastern, central, and southern genetic group, respectively), (b) photos of natural *Quercus mongolica* habitats under different environmental conditions, and (c) point clouds of individual *Q. mongolica* trees under different environmental conditions. The topographic and climate conditions of each site are listed in Table S1.

Three to five mature *Q. mongolica* trees were randomly selected within each plot. Their DBH and crown base height were measured using a diameter tape and a laser range finder, and their age was measured by coring each tree at a height of 1.3 m above the ground in the north-south cardinal direction. Besides, around 80 individual leaves without any damage were collected from each plot using a tree pruner. We made sure that these leaves were collected from different height strata and the ratio of shadow leaves to sun leaves in each plot were around 1:1. Each leaf was first measured by a caliper to derive the leaf thickness and then was digitized by a Canon LiDE 220 scanner. The scanned image of each leaf was processed by the software of WinFOLIA to estimate its area and vein length. Finally, each individual leaf was dried and weighted to calculate its specific leaf area (Table 1). Note that tree age measurements were not collected in sites N1, E1, E2, and E3 due to the malfunction of the increment borer in sites N1 and E2 and the unfortunate loss of tree cores in E1 and E3 during shipment. All leaf-related measurements were not collected in site C2 because its data collection time was in early spring, and leaves were still in the early-development stage, and leaf thickness was not collected in sites N3 and C1 because the data collection time was in early fall, and leaves had been in the process of turning yellow.

2.4. Individual Tree Segmentation From TLS Data

Individual tree segmentation is a prerequisite step for estimating individual tree parameters from TLS data (Li et al., 2012). In this study, a point cloud-based individual tree segmentation algorithm proposed by Tao, Wu, et al. (2015) was adopted. This algorithm first uses the points 10–30 cm above the ground to create a point density map and then uses the DBSCAN (density-based spatial clustering of applications with noise)

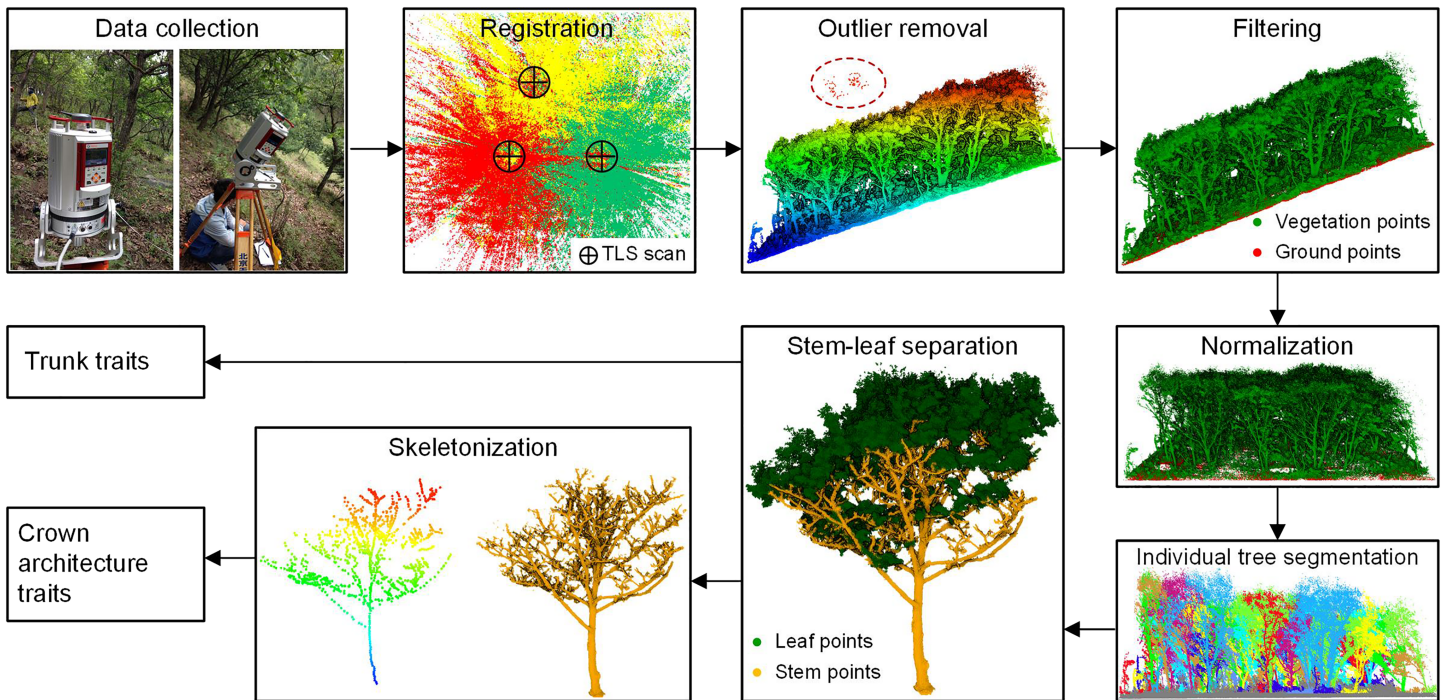


Figure 3. Illustration of the steps for TLS data acquisition, preprocessing, and architecture traits extraction.

algorithm to search the kernel point of each cluster. These kernel points are used as the seed points, and the distances of an unlabeled point to these seed points are compared by using the comparative shortest-path algorithm. The seed point with the shortest path to this point is labeled as the same tree. This process is repeated until all points being labeled.

By matching with field records, all *Q. mongolica* trees in each plot were extracted from the individual tree segmentation results (Figure 3). The point cloud of each *Q. mongolica* tree was visually examined and

Table 1

The list of trunk, crown, and leaf traits used in this study and their corresponding derivation data sources and methods

Traits	Source	Derivation method
a. Trunk traits		
Height	TLS data	Maximum height-ground height
Diameter at breast height	TLS data	Circle fitting method
b. Crown architecture traits		
Leaf area index	TLS data	Algorithm proposed by Li et al. (2017)
Live crown ratio	TLS data	(Height-crown base height)/height
Apical dominance ratio	TLS data	Height/crown diameter
Crown shape ratio	TLS data	(Height-crown base height)/crown diameter
Primary branch insertion angle	TLS data	Direct measurement
Bifurcation ratio	TLS data	Secondary:Primary branch number
Primary branch diameter ratio	TLS data	Primary branch diameter: DBH
Branch diameter ratio	TLS data	Secondary:Primary branch diameter
Chord length ratio	TLS data	Secondary:Primary branch chord length
c. Leaf traits		
Leaf thickness	Field data	Direct measurement
Leaf area	Field data	Direct measurement
Leaf vein length	Field data	Direct measurement
Specific leaf area	Field data	Leaf area/dry leaf weight

Note. TLS represents the terrestrial laser scanning.

corrected if there were points mislabeled. Moreover, if the point cloud of a *Q. mongolica* tree was incomplete due to the occlusion of branches and leaves, the corresponding tree was removed from the following analysis. Finally, each study site had 15–30 *Q. mongolica* trees reserved for the following analyses.

2.5. Trunk and Crown Traits Extraction From TLS Data

Trunk and crown traits were estimated from the segmented TLS data (Table 1). Tree height was computed as the height difference between the highest point of a tree and the ground, and DBH was calculated by fitting a circle to the points with a height of 1.3 m above the ground (Liang et al., 2016). Leaf area index (LAI) was estimated using a point cloud slicing-based algorithm proposed by Li et al. (2017). This algorithm first slices the point cloud based on an incident zenith angle of 5° and then derives gap fraction and clumping index based on the sliced point cloud. The Beer-Lambert Law is finally used to calculate the LAI from the derived gap fraction and clumping index. Crown base height, crown diameter, and tree height were the inputs for estimating the three crown shape-related traits (including live crown ratio, apical dominance ratio, and crown shape ratio) (Table 1). In this study, the canopy base height was calculated using an inflection point detection-based algorithm (Luo et al., 2018). This method assumes that if there were no other low vegetation under a tree, the height of the first inflection point of a tree's TLS percentile distribution curve is the crown base height. To calculate the crown diameter, we first used the Graham scanning algorithm to find the convex hull from the tree crown points (Graham, 1972), and the diameter of the fitted circle of the convex hull was used as the crown diameter. The three crown shape-related architecture traits were finally computed from the estimated crown base height, crown diameter, and tree height using the corresponding equations in Table 1.

To estimate the crown architecture traits related to the branching form (including primary branch insertion angle, bifurcation ratio, primary branch diameter ratio, branch diameter ratio, and chord length ratio), we first manually separated leaf and stem points using the LiDAR360 software (Figure 3) and then delineated the skeleton of each tree from the TLS data using a geometry-based algorithm (Tao, Guo, et al., 2015). The extracted tree skeletons were visually examined and corrected if there were any stems/branches missing. The number of branches at each order, the insertion angle of primary branches, and the length, diameter, and chord length of each branch were manually measured from the skeletons using the LiDAR360 software, which were then used to calculate the abovementioned traits using the corresponding equations in Table 1. It should be noted that we only drew the skeletons up to the secondary branch with a diameter ≥ 3 cm. Third-order branches or branches with a diameter < 3 cm were excluded because most of them were incomplete in the TLS point cloud due to the occlusion effect. Therefore, the bifurcation ratio, ratio of branch diameter, and chord length ratio used in this study all represented the ratios between the secondary branches and primary branches.

2.6. Statistical Analysis

The nested ANOVA (analysis of variance), a statistical method that can test whether there are significant variations in means among groups, subgroups within groups, etc. (Sokal & Rohlf, 1969), was used to analyze whether the geographical variation of each tree attribute was statistically significant between genetic groups and between populations within genetic groups. In this study, a two-level nested ANOVA was used, and the null hypothesis of each level was that there was no significant difference in the means of each tree attribute. Moreover, the linear regression methods were further used to evaluate whether tree attributes had spatial patterns along the latitude, longitude, and altitude gradients, and the statistical *t*-test was used to determine the significance level of each correlation. Note that we used the site-average values of each attribute to perform the linear regression analysis.

Two climate variables, that is, MAT and MAP, were used to evaluate the acclimation of trunk, crown, and leaf traits to the climate variability. The climate data were obtained from the National Meteorological Information Center of China. The 1960–2014 monthly average temperature and total precipitation were used to calculate the MAT and MAP of each study site. We assumed that if a trait showed acclimation to the climate variability, it should have strong correlations with the climate variables. Therefore, we calculated the Pearson's correlation coefficient to evaluate the correlations between a trait and climate variables, and the statistical *t*-test was used to determine the significance level of each correlation.

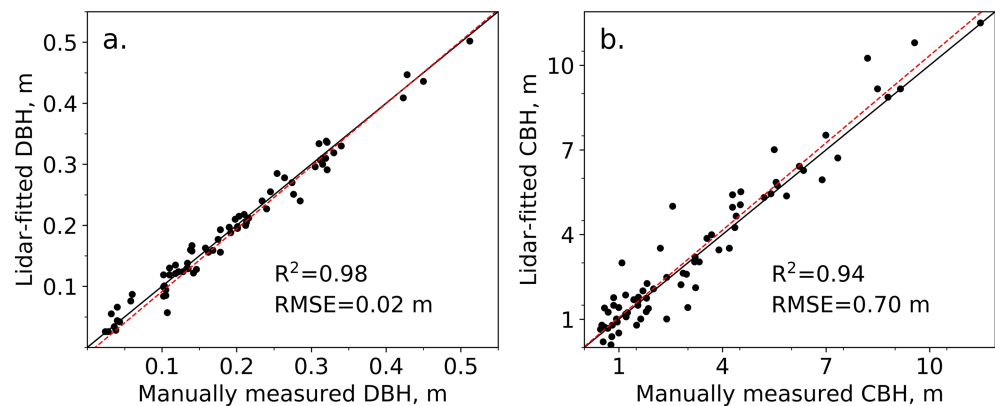


Figure 4. Accuracy assessment for the (a) terrestrial laser scanning (TLS)-derived diameter at breast height (DBH) and (b) TLS-derived crown base height (CBH). The red dashed line represents the fitted line, and the black solid line represents the 1:1 line. R^2 and RMSE represent the coefficient of determination and root-mean-square error, respectively.

The coordinated effect between crown architecture traits and trunk and leaf traits were first evaluated by calculating the Pearson's correlation coefficients between them as well. Besides, we further used the structure equation modelling (SEM) method to quantify the coordinated effects between crown architecture traits and trunk and leaf traits to the climate variability. SEM is a multivariate casual modelling technique that combines confirmatory factor analysis and multiple regression analysis (Kline, 2015). It allows users to quantify all path coefficients, which has been widely used in ecological studies to determine the logical and methodological relationship between correlation and causation (Fan et al., 2016; Maddox & Antonovics, 1983). In this study, we only built SEM models for the crown architecture traits showing strong correlations with the climate variability. To simplify the SEM models, tree height and specific leaf area were used to represent trunk traits and leaf traits, since they had similar correlations with the climate variability as other trunk and leaf traits. All input parameters were transformed with a logistic function to ensure them following normal distributions. The maximum likelihood method was used to estimate the standard path coefficients, and the significance of each path coefficient was calculated. Adequacy of the SEM models were evaluated by the comparative fit index (CFI) and the standardized root mean square residual (SRMR). High CFI (>0.8) and low SRMR (<0.08) indicate there is no difference between the observed covariance and modelled covariance, and therefore, the model could be accepted (Kline, 2015). Note that since leaf trait measurements could not match with trunk and crown trait measurements at the individual tree level in this study, we repeated the average trait measurements in each study site for the times of number of trees in each study site to build SEM models.

The nested analysis ANOVA, linear regression, and SEM analyses in this study were all performed using the R statistical programming language.

3. Results

3.1. Spatial Variations of Trunk, Crown, and Leaf Traits

Trunk traits and crown architecture traits were extracted from the TLS data through the procedure of registration, denoising, ground point filtering, normalization, and individual tree segmentation, and leaf traits were acquired through field measurements. The individual tree segmentation accuracy from TLS data were higher than 75% for all 12 study sites (Figure S1), and the estimated DBH and crown base height were highly correlated with ground truth measurements ($R^2 > 0.98$) (Figure 4). The estimated trunk, crown, and leaf traits showed substantial variations spatially (Figure S2). All traits used in this study showed significant differences among genetic groups with p values smaller than 0.001, except apical dominance ratio, primary branch diameter ratio, and chord length ratio (Table 2). Apical dominance ratio and primary branch diameter showed significant variations among genetic groups at the confidence level of 95%, and chord length ratio showed insignificant variations among genetic groups ($p > 0.05$) (Table 2). Within genetic groups, over 60% of the traits still showed significant variations ($p < 0.05$) among study sites. The study sites with insignificant trait variations were concentrated in the eastern and southern genetic groups (Table 2).

Table 2
The significance of variations of tree attributes among genetic groups and among study sites

Attributes	Significance		Parameters	Significance	
	Genetic group	Site		Genetic group	Site
Age	ns	N: ** E: NA C: *** S: ***	Bifurcation ratio	***	N: *** E: *** C: *** S: ns
Height	***	N: *** E: *** C: *** S: ***	Primary branch diameter ratio	*	N: *** E: *** C: *** S: *
DBH	***	N: *** E: *** C: *** S: ns	Branch diameter ratio	***	N: *** E: *** C: *** S: ns
Leaf area index	***	N: *** E: *** C: ns S: ***	Chord length ratio	ns	N: * E: ns C: ns S: ns
Live crown ratio	***	N: *** E: *** C: *** S: ns	Leaf thickness	***	N: *** E: ns C: NA S: ***
Apical dominance ratio	*	N: *** E: *** C: *** S: *	Leaf area	***	N: *** E: ns C: * S: ***
Crown shape ratio	***	N: *** E: *** C: *** S: *	Leaf vein length	***	N: *** E: ns C: ns S: ***
Primary branch insertion angle	***	N: ns E: *** C: *** S: ***	Specific leaf area	***	N: *** E: ns C: ** S: **

NA represents that the significance level cannot be calculated due to the missing of data at the correspond site. ns represents the variation is not significant.

*the variation is significant at the confident level of 95%. **the variation is significant at the confident level of 99%.

***the variation is significant at the confident level of 99.9%.

We explored the spatial distribution pattern of leaf, trunk, and crown traits along longitude, latitude, and altitude (Figure 5). Except the significant relationships between longitude and altitude with leaf traits, we did not observe any other significant spatial distribution pattern. Although LAI showed a decreasing trend from west to east and tree height and DBH showed increasing trends from low to high altitude, the p values of these correlations were larger than 0.05 (Figures 5a and 5c). Three out of the four leaf traits (i.e., leaf area, leaf vein length, and specific leaf area) showed significant increasing trends from west to east and significant decreasing trends from low to high altitude ($p < 0.05$) (Figures 5a and 5c). Leaf thickness had opposite changing patterns along the longitude and altitude gradients, although the correlations were not statistically significant (Figures 5a and 5c).

3.2. Climatic Controls on Trunk, Crown, and Leaf Traits

We evaluated the acclimation of trunk, crown, and leaf traits to the climate variability by calculating the Pearson's correlation coefficients with MAT and MAP (Figure 6). Overall, temperature showed no significant correlations with trunk and leaf traits. Although there were positive trends between leaf area/leaf vein length and MAT, the p values were larger than 0.1 (Figure 6a). However, temperature showed stronger correlations with certain crown architecture traits than with trunk and leaf traits. Crown shape ratio and chord length ratio were the only two traits significantly correlated with MAT. Besides, apical dominance ratio and

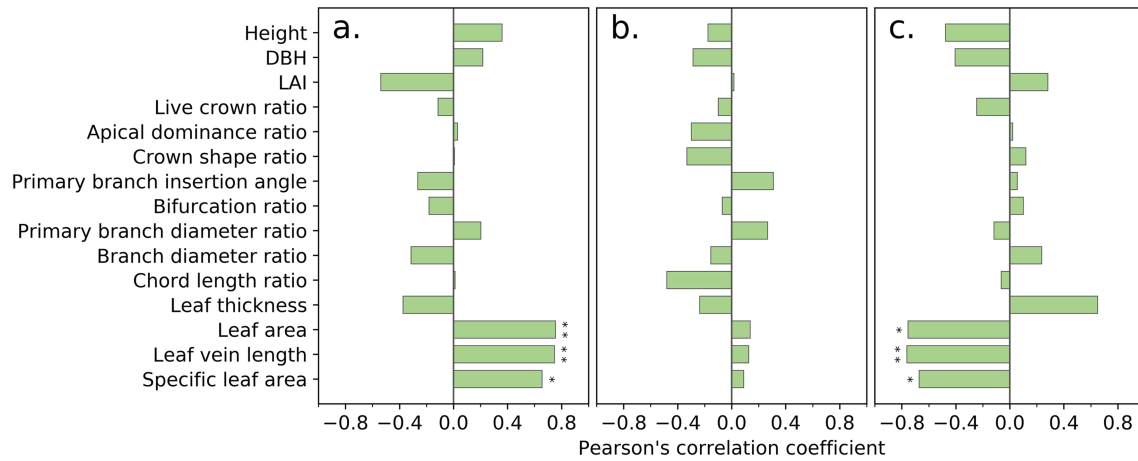


Figure 5. The Pearson's correlation coefficient between estimated traits and (a) longitude, (b) latitude, and (c) altitude. If a correlation is significant, the corresponding bar is labeled as ***, **, or *, indicating a confident level of 99.9%, 99%, or 95%, respectively.

primary branch insertion angle also showed strong correlations with MAT with p values smaller than 0.06 (Figure 6a).

Precipitation showed stronger influences on trunk and leaf traits than temperature. All trunk and leaf traits (except leaf thickness) showed significant positive correlations with MAP ($R > 0.7$) (Figure 6b), suggesting the increasing water availability could lead *Q. mongolica* trees to larger stature and larger leaves. Although the correlation was insignificant, the correlation coefficient between leaf thickness and MAP still reached -0.58 (Figure 6b). The negative correlation between leaf thickness and MAP suggested the leaf thickness tended to increase in areas with severer water deficiency. Among all the crown architecture traits, LAI, primary branch insertion angle, and chord length ratio were the only three having significant correlations with MAP (Figure 6b). LAI and primary branch insertion angle were negatively correlated to MAP, while chord length ratio was positively correlated to MAP. Apical dominance ratio and crown shape ratio also showed positive correlations with MAP, and the corresponding correlation coefficients were larger than 0.5 with the p values smaller than 0.1.

3.3. Coordination of Crown Architecture Traits to Trunk and Leaf Traits

The coordination of crown architecture traits to trunk and leaf traits were evaluated by the Pearson's correlation coefficients between them. Among all crown architecture traits, LAI, primary branch insertion angle,

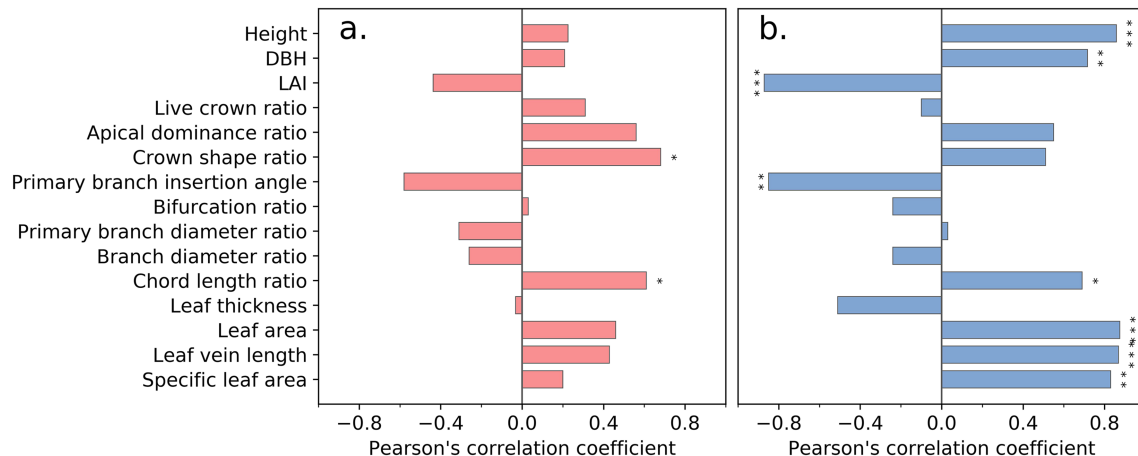


Figure 6. The Pearson's correlation coefficients between estimated traits and (a) mean annual temperature (MAT) and (b) MAP. If a correlation is significant, the corresponding bar is labeled as ***, **, or *, indicating a confident level of 99.9%, 99%, or 95%, respectively.

	Height	DBH	Leaf thickness	Leaf area	Leaf vein length	Specific leaf area
LAI	-0.87	-0.81	0.68	-0.76	-0.76	-0.69
Live crown ratio	-0.30	-0.04	-0.13	0.09	0.09	-0.26
Apical dominance ratio	0.44	-0.01	-0.40	0.34	0.31	0.36
Crown shape ratio	0.32	-0.06	-0.39	0.37	0.33	0.28
Primary branch insertion angle	-0.81	-0.56	0.61	-0.59	-0.58	-0.65
Bifurcation ratio	-0.21	0.03	0.64	-0.37	-0.41	-0.32
Primary branch diameter ratio	0.20	0.30	-0.78	0.02	0.10	-0.06
Branch diameter ratio	-0.09	0.08	0.38	-0.37	-0.32	-0.22
Chord length ratio	0.67	0.61	-0.67	0.47	0.44	0.54

Figure 7. The Pearson's correlation coefficient between crown architecture traits and tree- and leaf-level architecture traits. Blocks in reddish colors represent a positive correlation, and blocks in blueish colors represent a negative correlation. Note that LAI represents the leaf area index.

and chord length ratio were the only three traits showing strong correlations with all trunk and leaf traits (Figure 7). LAI and primary branch insertion angle were positively correlated with all trunk and leaf traits (except leaf thickness), while chord length ratio was negatively correlated with them. Beyond the above three crown architecture traits, only bifurcation ratio and primary branch diameter ratio had an absolute correlation coefficient with leaf thickness larger than 0.6 (Figure 7). The strong correlations between selected crown architecture traits and trunk/leaf traits suggested that there were coordinated effects between crown architecture traits and trunk and leaf traits.

We further examined how climate variability mediates the coordinated variations among leaf, crown, and branch traits using the SEM method. Here, we simplified the SEM models by using tree height and specific leaf area to represent trunk and leaf traits, respectively, since they had similar responses to the climate variability as other trunk and leaf traits (Figure 6). Moreover, we here only presented SEM models for four crown architecture traits having significant correlations with MAP and/or MAT (i.e., LAI, crown shape ratio, primary branch insertion angle, and crown length ratio). As can be seen in Figure 8, all four models had CFIs larger than 0.95 and SRMRs smaller than 0.08, indicating that they could be accepted statistically.

Similar as the findings presented in Figure 6, MAP had the largest contributions to the variabilities in tree height and specific leaf area. The path coefficients (β) from MAP to tree height and specific leaf area were the largest among all path coefficients at the corresponding nodes for all four SEM models (Figure 8). MAT had more profound influences on the variations of crown architecture traits (except LAI). The path coefficients from MAT to crown shape ratio and chord length ratio were larger than those from MAP to

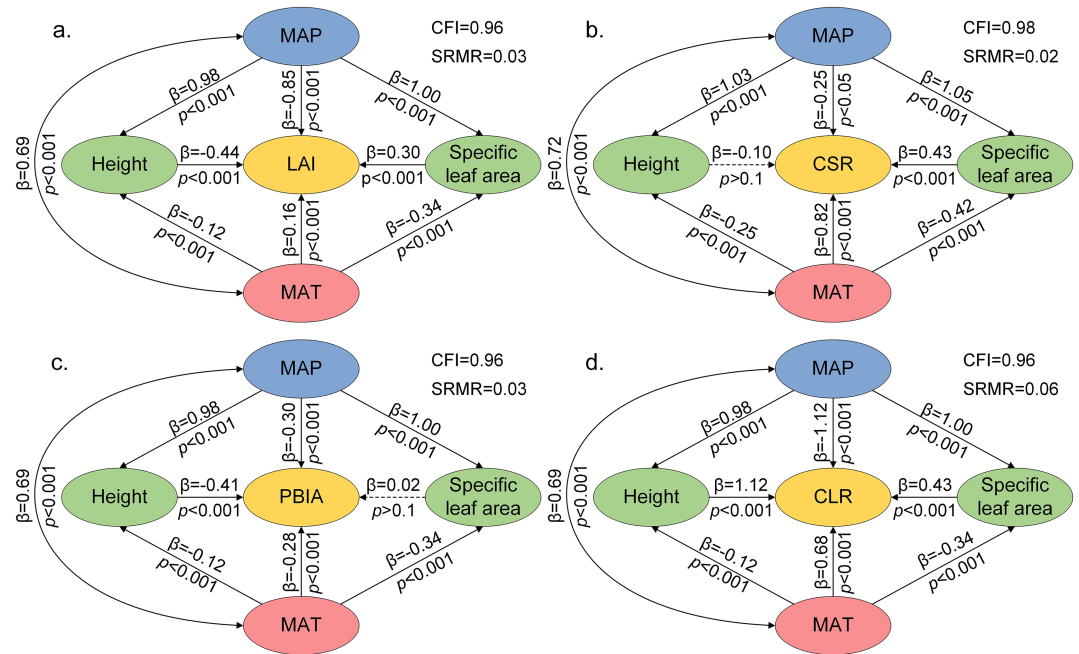


Figure 8. The coordination of (a) LAI, (b) crown shape ratio (CSR), (c) primary branch insertion angle (PBI), and (d) chord length ratio (CLR) to tree height, specific leaf area, MAP, and MAT demonstrated by structure equation models. Note that β represents the path coefficient, p represents the p value of the path, CFI represents the comparative fit index, and SRMR represents the standardized root mean square residual.

them (Figures 8b and 8d). Besides climate variables, crown architecture traits showed significant coordination to tree height and/or specific leaf area. LAI was negatively correlated with tree height ($\beta = -0.44, p < 0.001$), while positively correlated with specific leaf area ($\beta = 0.3, p < 0.001$) (Figure 8a). Crown shape ratio was not significantly influenced by tree height ($p > 0.1$) but had a significant positive correlation with specific leaf area ($\beta = -0.43, p < 0.001$) (Figure 8b). Primary branch insertion angle was negatively influenced by tree height ($\beta = -0.41, p < 0.001$) while had no significant correlation with specific leaf area ($p > 0.1$) (Figure 8c). Chord length ratio was positively correlated with tree height, and the path coefficient was the largest among all factors (Figure 8d). However, it had no significant correlation with the specific leaf area ($p > 0.1$) (Figure 8d).

4. Discussion

In this study, 15 trunk, crown, and leaf traits were selected by considering the possibility of being measured (either from the field or from TLS data) and the importance to define tree architecture (Ceulemans et al., 1990; Lau et al., 2018). Both the empirical and statistical analyses demonstrate that trunk, crown, and leaf traits of *Q. mongolica* trees have significant spatial variations, even within the same genetic group (Figure S2, Table 2). There are no significant differences in tree age among genetic groups (Table 2), suggesting that the differences in trunk, crown, and leaf traits are not caused by tree age differences. Moreover, only leaf size-related traits (i.e., leaf area, leaf vein length, and specific leaf area) show significant changing patterns along the altitude and latitude axes (Figure 5). The correlations between geographical factors and these leaf traits might be manipulated by the change of precipitation. MAP has a significant positive correlation with longitude and a significant negative correlation with altitude (Figure S3), which are in correspondence with the correlations between MAP and leaf traits (Figure 6b). This indicates that the control of geographical attributes (i.e., latitude, longitude, and altitude) on a tree architecture trait is dependent on the influence of climatic factors and might be the result of an integrated effect of multiple climatic factors.

All trunk and leaf traits strongly acclimate to the MAP gradients, and the findings are consistent with previous studies that trees tend to grow taller and have larger leaves in wetter areas (Tao et al., 2016; Wright et al., 2017). No trunk and leaf traits show significant correlations with MAT, indicating that the trunk

and leaf growth of *Q. mongolica* trees in the study sites are more constrained by precipitation instead of temperature. This might explain why most traits with insignificant variations among study sites are found in eastern and southern genetic groups (Table 2). These two groups are distributed in semihumid and humid areas (Figure 2a), which might be less limited by water availability (Lyu et al., 2017; Zhu et al., 2018). Therefore, genetic information might have a more profound influence on the formation of tree trunks and leaves, leading to relatively small variations in them. Over a half of the nine crown architecture traits in this study do not have significant correlations with the climate variability (Figure 6). West et al. (2009) and Enquist et al. (2009) proposed that tree branching followed a general quantitative theory, and Bentley et al. (2013) further suggested that tree branching network followed allometric scaling relationships, which indicate that certain crown architecture traits might have low plasticity (Figure S4) and be more controlled by genetic information instead of environmental conditions.

The coordinated effects among crown architecture traits, trunk traits, leaf traits, MAT, and MAP further help to explain the hydraulic constraints and defensive strategies of trees to the increasingly drier environment in northern China (Xu et al., 2010). The variations in LAI are influenced by the coordination among MAP, tree height, LAI, and specific leaf area. The total contribution of MAT to LAI is much smaller than that of MAP to LAI (Figure 8a). With the increase of MAP, LAI has a significant decreasing pattern, although the size of a single leaf has a significant increasing pattern (Figure 6b). This may be partly caused by the negative feedback of the paths from MAP to tree height to LAI (Figure 8a). The increase of MAP can increase the vertical space of a tree by increasing tree height, making the interleaf gaps become larger, and therefore reducing the LAI values (Li et al., 2016). This suggests that *Q. mongolica* trees may have evolution strategies to balance leaf size and interleaf gap size to minimize self-shading and therefore achieve optimal resource-use (i.e., light-use and water-use) efficiencies. The variations in crown shape ratio are the mixing effect among MAP, MAT, and specific leaf area. With the increase of MAT, *Q. mongolica* trees tend to increase self-shading by narrowing their crowns (Figure 8b), which can reduce per-leaf-area water loss via plant transpiration to avoid the higher atmospheric water deficit stress (that is positively related with high temperature) (Gignoux et al., 2016; Kuuluvainen & Pukkala, 1987). Meanwhile, the higher temperature has negative effect on the specific leaf area (Figure 8b), which varies in accordance with the change in crown shape ratio to reduce water loss (Wright et al., 2017). With the increase of MAP, *Q. mongolica* trees tend to expand the crown size and increase the leaf size to maximize the light capture (Sterck et al., 2001; Wright et al., 2005) (Figure 8b). Primary branch insertion angle and chord length ratio change accordingly with tree height and specific leaf area in response to the climate variability. With the increase of MAP, *Q. mongolica* trees tend to grow taller and vertical vegetation layering might emerge, which makes light resources to become increasingly important limitations to tree growth (Dong et al., 2012). Therefore, they tend to decrease primary branch insertion angles and increase chord length ratios (Figures 8c and 8d) to create tree shapes like the rightmost tree in Figure 2c to maximize light capture (Davies & Ashton, 1999; Sterck et al., 2001; Wright et al., 2005). With the increase of MAT, *Q. mongolica* trees tend to decrease primary branch insertion angles (Figures 8c and 8d) and create crown shapes like the four trees on the left of Figure 2c to alleviate the water loss (Gignoux et al., 2016; Kuuluvainen & Pukkala, 1987). Meanwhile, the specific leaf area also changed correspondingly to increase the photosynthesis or reduce transpiration (Wright et al., 2017).

With the observed tight coordinated variations among crown architecture traits, trunk traits, leaf traits, and climate variations, we further hypothesize that crown architecture might have a “bridging” effect between the water and light demands of *Q. mongolica* trees. In a relatively moister climatic area, *Q. mongolica* trees have the potential to reach a larger stature (Figure 6b), which requires a higher light demand. To maximize the biomass production, crown architecture might serve as the regulator of light capture by quickly increasing the ratio of crown and growing more upward (Craine & Dybzinski, 2013). In a relatively drier climatic area, *Q. mongolica* trees tend to have a smaller stature due to the water limitation (Figure 6b), and therefore, crown architecture tends to grow horizontally to increase biomass production by improving water-use efficiency. In a relatively hotter climatic area, crown architecture of *Q. mongolica* trees tends to develop vertically to create self-shading to reduce water loss via plant transpiration (Gignoux et al., 2016; Kuuluvainen & Pukkala, 1987) (Figure 6a). While in a colder climatic area, crown architecture of *Q. mongolica* trees tends to structure branches horizontally to maximize light capture (Figure 6a). The potential strategy of *Q.*

mongolica trees balancing the water and light demands through the coordination of crown and leaf traits can help to understand the mechanism of how plants reduce to opportunity cost to balance storage, accumulation, and recycling (Chapin et al., 1990)

With the prediction of warmer and drier semiarid areas (Greve et al., 2014), we can predict that *Q. mongolica* trees might have a trend of shifting from “tree shape” (i.e., larger tree height and DBH, larger and thinner leaf, and larger crown with vertical development) to “shrub shape” (i.e., smaller tree height and DBH, smaller and thicker leaf, and smaller crown with horizontal development) to maintain biomass production. However, current dynamic global vegetation models usually estimate crown area by tree height and rarely consider the acclimation of crown architecture traits to the climate variability (Hickler et al., 2006; Sitch et al., 2003), which might bring significant underestimation in the canopy coverage in semiarid areas. The coordinated variations among crown architecture, trunk, and leaf traits with the large-scale variability in climate as observed in this study highlight the importance of including this finding into future vegetation dynamic modelling studies. Moreover, future studies are still needed to identify key crown traits indicating tree architecture variations and coordinating with trunk and leaf traits to help improve dynamic global vegetation models.

The lack of efficient and accurate methods to obtain repeatable crown architecture observations has long been a bottleneck in the field of crown architecture studies (Malhi et al., 2018). The rich and accurate three-dimensional information provided by TLS data has made the estimation of crown architecture traits in a repeatable and accurate manner become possible over large spatial scales in this study. Although manual efforts are still needed to examine the results, it still provides an effective and accurate way to derive crown architecture traits with much less labor and time involved. Currently, the most time-consuming and labor-intensive process in TLS-based method is the TLS data collection and registration. With the development of terrestrial mobile systems (e.g., backpack TLS and handheld TLS), the efficiency of TLS data collection can be significantly improved, and there is no need for data registration anymore (Liang et al., 2014; Qian et al., 2017), which can further improve the efficiency of estimating crown architecture traits. Moreover, the present study only tested the workflow and methodology on one tree species, that is, *Q. mongolica* tree, considering its dramatic variations in tree architecture under different climate conditions (Kitao et al., 2000; Kitao et al., 2006). However, we believe that they have the potential to be applied on study the tree architecture of other tree species, especially considering the recent technical advances in automatically extracting crown traits from TLS data (Bremer et al., 2018; Lau et al., 2018).

5. Conclusions

In summary, this study evaluates the geographical variations of and climatic controls on trunk, crown, and leaf traits of *Q. mongolica* trees over large spatial scales in northern China. Our results show that trunk, crown, and leaf traits have substantial variations over space, but only leaf traits have significant correlations with longitude and latitude. Five out of the six trunk and leaf traits show sensitive responses to the precipitation variability. Generally, larger-stature *Q. mongolica* trees with larger and thinner leaves are more likely to occur at areas with higher precipitation. Half of the selected crown architecture traits show acclimation to variations in MAT and/or MAP, and they have strong coordinated effects with trunk and leaf traits. As the bridge linking tree trunk and leaves, crown architecture traits play a significant role in balancing the water and light demands of a tree. The results of this study show the significance of long-neglected crown architecture traits in the evolutionary strategy of a tree. Although the current study only focuses on one tree species from semihumid and semiarid areas, the proposed method can be applied on other species in other areas, which will ultimately allow us to have a better understanding on how trees may evolve under the background of global climate change and how the coordinated effects of crown architecture traits may influence the global carbon cycling simulation.

References

- Bennett, A. C., McDowell, N. G., Allen, C. D., & Anderson-Teixeira, K. J. (2015). Larger trees suffer most during drought in forests worldwide. *Nature Plants*, *1*(10), 15139. <https://doi.org/10.1038/nplants.2015.139>
- Bentley, L. P., Stegen, J. C., Savage, V. M., Smith, D. D., von Allmen, E. I., Sperry, J. S., et al. (2013). An empirical assessment of tree branching networks and implications for plant allometric scaling models. *Ecology Letters*, *16*(8), 1069–1078. <https://doi.org/10.1111/ele.12127>

Acknowledgments

This work was supported by the Frontier Science Key Programs of the Chinese Academy of Sciences (QYZDY-SSW-SMC011), National Natural Science Foundation of China (41871332, 31971575, 41790422, 41530747), and the CAS Pioneer Hundred Talents Program. The climate data are obtained from the National Meteorological Information Center of China (<http://data.cma.cn/en>). The data used to analyze the spatial variations and climatic controls of *Q. mongolica* crown architecture traits can be freely accessed through the open repository figshare (<https://doi.org/10.6084/m9.figshare.11836698.v1>).

- Bremer, M., Wichmann, V., & Rutzinger, M. (2018). Multi-temporal fine-scale modelling of Larix decidua forest plots using terrestrial LiDAR and hemispherical photographs. *Remote Sensing of Environment*, 206, 189–204.
- Calders, K., Disney, M. I., Armston, J., Burt, A., Brede, B., Origo, N., et al. (2017). Evaluation of the range accuracy and the radiometric calibration of multiple terrestrial laser scanning instruments for data interoperability. *IEEE Transactions on Geoscience and Remote Sensing*, 55(5), 2716–2724.
- Calders, K., Newnham, G., Burt, A., Murphy, S., Raunonen, P., Herold, M., et al. (2015). Nondestructive estimates of above-ground biomass using terrestrial laser scanning. *Methods in Ecology and Evolution*, 6(2), 198–208.
- Ceulemans, R., Stettler, R. F., Hinckley, T. M., Isebrands, J. G., & Heilman, P. E. (1990). Crown architecture of Populus clones as determined by branch orientation and branch characteristics. *Tree Physiology*, 7(1-2-3-4), 157–167.
- Chapin, F. S. III, Schulzeand, E. D., & Mooney, H. A. (1990). The ecology and economics of storage in plants. *Annual Review of Ecology and Systematics*, 21(1), 423–447.
- Chave, J., Andalo, C., Brown, S., Cairns, M. A., Chambers, J. Q., Eamus, D., et al. (2005). Tree allometry and improved estimation of carbon stocks and balance in tropical forests. *Oecologia*, 145(1), 87–99. <https://doi.org/10.1007/s00442-005-0100-x>
- Craine, J. M., & Dybzinski, R. (2013). Mechanisms of plant competition for nutrients, water and light. *Functional Ecology*, 27(4), 833–840.
- Dassot, M., Constant, T., & Fournier, M. (2011). The use of terrestrial LiDAR technology in forest science: application fields, benefits and challenges. *Annals of Forest Science*, 68(5), 959–974.
- Davies, S. J., & Ashton, P. S. (1999). Phenology and fecundity in 11 sympatric pioneer species of Macaranga (Euphorbiaceae) in Borneo. *American Journal of Botany*, 86(12), 1786–1795.
- Disney, M. (2018). Terrestrial LiDAR: A three-dimensional revolution in how we look at trees. *New Phytologist*, 222(4), 1736–1741.
- Dong, S. X., Davies, S. J., Ashton, P. S., Bunyavejchewin, S., Supardi, M. N. N., Kassim, A. R., et al. (2012). Variability in solar radiation and temperature explains observed patterns and trends in tree growth rates across four tropical forests. *Proceedings of the Royal Society B: Biological Sciences*, 279(1744), 3923–3931. <https://doi.org/10.1098/rspb.2012.1124>
- Enquist, B. J., West, G. B., & Brown, J. H. (2009). Extensions and evaluations of a general quantitative theory of forest structure and dynamics. *Proceedings of the National Academy of Sciences*, 106(17), 7046–7051.
- Escudero, A., Del Río, T., Sánchez-Zulueta, P., & Mediavilla, S. (2017). Ontogenetic changes in crown architecture and leaf arrangement: Effects on light capture efficiency in three tree species differing in leaf longevity. *Ecological Research*, 32(4), 595–602.
- Fan, Y., Chen, J., Shirkey, G., John, R., Wu, S. R., Park, H., & Shao, C. (2016). Applications of structural equation modeling (SEM) in ecological studies: An updated review. *Ecological Processes*, 5(1), 19.
- Forrester, D. I., Ammer, C., Annighöfer, P. J., Barbeito, I., Bielak, K., Bravo-Oviedo, A., et al. (2018). Effects of crown architecture and stand structure on light absorption in mixed and monospecific Fagus sylvatica and Pinus sylvestris forests along a productivity and climate gradient through Europe. *Journal of Ecology*, 106(2), 746–760.
- Fortin, M., Van Couwenberghe, R., Perez, V., & Piedallu, C. (2018). Evidence of climate effects on the height-diameter relationships of tree species. *Annals of Forest Science*, 76(1), 1–20. <https://doi.org/10.1007/s13595-018-0784-9>
- Gignoux, J., Konaté, S., Lahoreau, G., Le Roux, X., & Simioni, G. (2016). Allocation strategies of savanna and forest tree seedlings in response to fire and shading: Outcomes of a field experiment. *Scientific Reports*, 6, 38838.
- Gonzalez de Tanago, J., Lau, A., Bartholomeus, H., Herold, M., Avitabile, V., Raunonen, P., et al. (2018). Estimation of above-ground biomass of large tropical trees with terrestrial LiDAR. *Methods in Ecology and Evolution*, 9(2), 223–234.
- Graham, R. L. (1972). An efficient algorithm for determining the convex hull of a finite planar set. *Information Processing Letters*, 1, 132–133.
- Greve, P., Orlowsky, B., Mueller, B., Sheffield, J., Reichstein, M., & Seneviratne, S. I. (2014). Global assessment of trends in wetting and drying over land. *Nature Geoscience*, 7(10), 716.
- Guisasola, R., Tang, X., Bauhus, J., & Forrester, D. I. (2015). Intra- and inter-specific differences in crown architecture in Chinese subtropical mixed-species forests. *Forest Ecology and Management*, 353, 164–172. <https://doi.org/10.1016/j.foreco.2015.05.029>
- Guo, Q., Li, W., Yu, H., & Alvarez, O. (2010). Effects of topographic variability and lidar sampling density on several DEM interpolation methods. *Photogrammetric Engineering & Remote Sensing*, 76(6), 701–712.
- Hallé, F., Oldeman, R. A., & Tomlinson, P. B. (1978). *Tropical trees and forests: An architectural analysis*. Berlin, Germany: Springer Science & Business Media.
- Hickler, T., Prentice, I. C., Smith, B., Sykes, M. T., & Zaehle, S. (2006). Implementing plant hydraulic architecture within the LPJ Dynamic Global Vegetation Model. *Global Ecology and Biogeography*, 15(6), 567–577.
- Iida, Y., Kohyama, T. S., Kubo, T., Kassim, A. R., Poorter, L., Sterck, F., & Potts, M. D. (2011). Tree architecture and life-history strategies across 200 co-occurring tropical tree species. *Functional Ecology*, 25(6), 1260–1268. <https://doi.org/10.1111/j.1365-2435.2011.01884.x>
- Ishii, H., & Asano, S. (2010). The role of crown architecture, leaf phenology and photosynthetic activity in promoting complementary use of light among coexisting species in temperate forests. *Ecological Research*, 25(4), 715–722. <https://doi.org/10.1007/s11284-009-0668-4>
- Jackson, T., Shenkin, A., Wellpott, A., Calders, K., Origo, N., Disney, M., et al. (2019). Finite element analysis of trees in the wind based on terrestrial laser scanning data. *Agricultural and Forest Meteorology*, 265(2), 137–144.
- Jin, S., Su, Y., Gao, S., Wu, F., Hu, T., Liu, J., et al. (2018). Deep learning: Individual maize segmentation from terrestrial lidar data using faster R-CNN and regional growth algorithms. *Frontiers in Plant Science*, 9. <https://doi.org/10.3389/fpls.2018.00866>
- Jin, S., Su, Y., Wu, F., Pang, S., Gao, S., Hu, T., et al. (2018). Stem-leaf segmentation and phenotypic trait extraction of individual maize using terrestrial lidar data. *IEEE Transactions on Geoscience and Remote Sensing*, 57(3), 1336–1346. <https://doi.org/10.1109/TGRS.2018.2866056>
- Kitao, M., Lei, T. T., Koike, T., Tobita, H., & Maruyama, Y. (2000). Susceptibility to photoinhibition of three deciduous broadleaf tree species with different successional traits raised under various light regimes. *Plant, Cell & Environment*, 23(1), 81–89. <https://doi.org/10.1046/j.1365-3040.2000.00528.x>
- Kitao, M., Lei, T. T., Koike, T., Tobita, H., & Maruyama, Y. (2006). Tradeoff between shade adaptation and mitigation of photoinhibition in leaves of *Quercus mongolica* and *Acer mono* acclimated to deep shade. *Tree Physiology*, 26(4), 441–448. <https://doi.org/10.1093/treephys/26.4.441>
- Kline, R. B. (2015). *Principles and practice of structural equation modeling* (Fourth edition ed.). New York, NY: Guilford publications.
- Kuuluvainen, T., & Pukkala, T. (1987). Effect of crown shape and tree distribution on the spatial distribution of shade. *Agricultural and Forest Meteorology*, 40(3), 215–231.
- Lau, A., Bentley, L. P., Martius, C., Shenkin, A., Bartholomeus, H., Raunonen, P., et al. (2018). Quantifying branch architecture of tropical trees using terrestrial LiDAR and 3D modelling. *Trees*, 32(5), 1219–1231.

- Lau, A., Martius, C., Bartholomeus, H., Shenkin, A., Jackson, T., Malhi, Y., et al. (2019). Estimating architecture-based metabolic scaling exponents of tropical trees using terrestrial LiDAR and 3D modelling. *Forest Ecology and Management*, *439*(5), 132–145.
- Li, W., Guo, Q., Jakubowski, M. K., & Kelly, M. (2012). A new method for segmenting individual trees from the lidar point cloud. *Photogrammetric Engineering & Remote Sensing*, *78*(1), 75–84.
- Li, Y., Guo, Q., Su, Y., Tao, S., Zhao, K., & Xu, G. (2017). Retrieving the gap fraction, element clumping index, and leaf area index of individual trees using single-scan data from a terrestrial laser scanner. *ISPRS Journal of Photogrammetry and Remote Sensing*, *130*, 308–316.
- Li, Y., Guo, Q., Tao, S., Zheng, G., Zhao, K., Xue, B., & Su, Y. (2016). Derivation, validation, and sensitivity analysis of terrestrial laser scanning-based leaf area index. *Canadian Journal of Remote Sensing*, *42*(6), 719–729.
- Li, Y., Su, Y., Hu, T., Xu, G., & Guo, Q. (2018). Retrieving 2-D leaf angle distributions for deciduous trees from terrestrial laser scanner data. *IEEE Transactions on Geoscience and Remote Sensing*, *56*(8), 4945–4955. <https://doi.org/10.1109/TGRS.2018.2843382>
- Liang, X., Hyypää, J., Kaartinen, H., Lehtomäki, M., Pyörälä, J., Pfeifer, N., et al. (2018). International benchmarking of terrestrial laser scanning approaches for forest inventories. *ISPRS Journal of Photogrammetry and Remote Sensing*, *144*, 137–179. <https://doi.org/10.1016/j.isprsjprs.2018.06.021>
- Liang, X., Hyypää, J., Kukko, A., Kaartinen, H., Jaakkola, A., & Yu, X. (2014). The use of a mobile laser scanning system for mapping large forest plots. *IEEE Geoscience and Remote Sensing Letters*, *11*(9), 1504–1508.
- Liang, X., Kankare, V., Hyypää, J., Wang, Y., Kukko, A., Haggren, H., et al. (2016). Terrestrial laser scanning in forest inventories. *ISPRS Journal of Photogrammetry and Remote Sensing*, *115*, 63–77.
- Luo, L., Zhai, Q., Su, Y., Ma, Q., Kelly, M., & Guo, Q. (2018). Simple method for direct crown base height estimation of individual conifer trees using airborne LiDAR data. *Optics Express*, *26*(10), A562–A578. <https://doi.org/10.1364/OE.26.00A562>
- Lusk, C. H., Grierson, E. R. P., & Laughlin, D. C. (2019). Large leaves in warm, moist environments confer an advantage in seedling light interception efficiency. *New Phytologist*, *223*(3), 1319–1327. <https://doi.org/10.1111/nph.15849>
- Lyu, S., Wang, X., Zhang, Y., & Li, Z. (2017). Different responses of Korean pine (*Pinus koraiensis*) and Mongolia oak (*Quercus mongolica*) growth to recent climate warming in northeast China. *Dendrochronologia*, *45*, 113–122. <https://doi.org/10.1016/j.dendro.2017.08.002>
- Maddox, G. D., & Antonovics, J. (1983). Experimental ecological genetics in *Plantago*: A structural equation approach to fitness components in *P. aristata* and *P. patagonica*. *Ecology*, *64*(5), 1092–1099.
- Magney, T. S., Eitel, J. U., Griffin, K. L., Boelman, N. T., Greaves, H. E., Prager, C. M., et al. (2016). LiDAR canopy radiation model reveals patterns of photosynthetic partitioning in an Arctic shrub. *Agricultural and Forest Meteorology*, *221*(5), 78–93.
- Malhi, Y., Jackson, T., Patrick Bentley, L., Lau, A., Shenkin, A., Herold, M., et al. (2018). New perspectives on the ecology of tree structure and tree communities through terrestrial laser scanning. *Interface Focus*, *8*(2), 20170052.
- Moorthy, I., Miller, J. R., Berni, J. A. J., Zarco-Tejada, P., Hu, B., & Chen, J. (2011). Field characterization of olive (*Olea europaea* L.) tree crown architecture using terrestrial laser scanning data. *Agricultural and Forest Meteorology*, *151*(2), 204–214. <https://doi.org/10.1016/j.agrformet.2010.10.005>
- Niinemets, Ü. (2001). Global-scale climatic controls of leaf dry mass per area, density, and thickness in trees and shrubs. *Ecology*, *82*(2), 453–469. [https://doi.org/10.1890/0012-9658\(2001\)082\[0453:GSCCOL\]2.0.CO;2](https://doi.org/10.1890/0012-9658(2001)082[0453:GSCCOL]2.0.CO;2)
- Ordoñez, J. C., Bodegom, P. M. V., Witte, J.-P. M., Wright, I. J., Reich, P. B., & Aerts, R. (2009). A global study of relationships between leaf traits, climate and soil measures of nutrient fertility. *Global Ecology and Biogeography*, *18*(2), 137–149. <https://doi.org/10.1111/j.1466-8238.2008.00441.x>
- Pearcy, R. W., Muraoka, H., & Valladares, F. (2005). Crown architecture in sun and shade environments: Assessing function and trade-offs with a three-dimensional simulation model. *New Phytologist*, *166*(3), 791–800. <https://doi.org/10.1111/j.1469-8137.2005.01328.x>
- Pearcy, R. W., Valladares, F., Wright, S. J., & de Paulis, E. L. (2004). A functional analysis of the crown architecture of tropical forest Psychotria species: Do species vary in light capture efficiency and consequently in carbon gain and growth? *Oecologia*, *139*(2), 163–177. <https://doi.org/10.1007/s00442-004-1496-4>
- Poorter, L., Bongers, F., Sterck, F. J., & Wöll, H. (2003). Architecture of 53 rain forest tree species differing in adult stature and shade tolerance. *Ecology*, *84*(3), 602–608. [https://doi.org/10.1890/0012-9658\(2003\)084\[0602:AORFTS\]2.0.CO;2](https://doi.org/10.1890/0012-9658(2003)084[0602:AORFTS]2.0.CO;2)
- Poorter, L., Bongers, L., & Bongers, F. (2006). Architecture of 54 moist-forest tree species: Traits, trade-offs, and functional groups. *Ecology*, *87*(5), 1289–1301. [https://doi.org/10.1890/0012-9658\(2006\)87\[1289:AOMTST\]2.0.CO;2](https://doi.org/10.1890/0012-9658(2006)87[1289:AOMTST]2.0.CO;2)
- Puttonen, E., Briese, C., Mandlburger, G., Wieser, M., Pfennigbauer, M., Zlinszky, A., & Pfeifer, N. (2016). Quantification of overnight movement of birch (*Betula pendula*) branches and foliage with short interval terrestrial laser scanning. *Frontiers in Plant Science*, *7*(2), 222.
- Qian, C., Liu, H., Tang, J., Chen, Y., Kaartinen, H., Kukko, A., et al. (2017). An integrated GNSS/INS/LiDAR-SLAM positioning method for highly accurate forest stem mapping. *Remote Sensing*, *9*(1), 3.
- Savage, V. M., Bentley, L. P., Enquist, B. J., Sperry, J. S., Smith, D. D., Reich, P. B., & von Allmen, E. I. (2010). Hydraulic trade-offs and space filling enable better predictions of vascular structure and function in plants. *Proceedings of the National Academy of Sciences*, *107*(52), 22,722–22,727.
- Sitch, S., Smith, B., Prentice, I. C., Arneeth, A., Bondeau, A., Cramer, W., et al. (2003). Evaluation of ecosystem dynamics, plant geography and terrestrial carbon cycling in the LPJ dynamic global vegetation model. *Global Change Biology*, *9*(2), 161–185.
- Sokal, R. R., & Rohlf, F. J. (1969). *The principles and practice of statistics in biological research*. New York: WH Freeman and company San Francisco.
- Sterck, F. J., Bongers, F., & Newbery, D. M. (2001). Tree architecture in a Bornean lowland rain forest: Intraspecific and interspecific patterns. *Plant Ecology*, *153*(1), 279–292. <https://doi.org/10.1023/A:1017507723365>
- Tao, S., Guo, Q., Li, C., Wang, Z., & Fang, J. (2016). Global patterns and determinants of forest canopy height. *Ecology*, *97*(12), 3265–3270.
- Tao, S., Guo, Q., Xu, S., Su, Y., Li, Y., & Wu, F. (2015). A geometric method for wood-leaf separation using terrestrial and simulated lidar data. *Photogrammetric Engineering & Remote Sensing*, *81*(10), 767–776.
- Tao, S., Wu, F., Guo, Q., Wang, Y., Li, W., Xue, B., et al. (2015). Segmenting tree crowns from terrestrial and mobile LiDAR data by exploring ecological theories. *ISPRS Journal of Photogrammetry and Remote Sensing*, *110*, 66–76.
- Thomas, S. C. (1996). Asymptotic height as a predictor of growth and allometric characteristics in Malaysian rain forest trees. *American Journal of Botany*, *83*(5), 556–566.
- Tingstad, L., Olsen, S. L., Klanderud, K., Vandvik, V., & Ohlson, M. (2015). Temperature, precipitation and biotic interactions as determinants of tree seedling recruitment across the tree line ecotone. *Oecologia*, *179*(2), 599–608. <https://doi.org/10.1007/s00442-015-3360-0>

- Valladares, F., & Pugnaire, F. I. (1999). Tradeoffs between irradiance capture and avoidance in semi-arid environments assessed with a crown architecture model. *Annals of Botany*, *83*(4), 459–469. <https://doi.org/10.1006/anbo.1998.0843>
- Vicari, M. B., Pisek, J., & Disney, M. (2019). New estimates of leaf angle distribution from terrestrial LiDAR: Comparison with measured and modelled estimates from nine broadleaf tree species. *Agricultural and Forest Meteorology*, *264*, 322–333.
- Wang, Y., Lehtomäki, M., Liang, X., Pyörälä, J., Kukko, A., Jaakkola, A., et al. (2019). Is field-measured tree height as reliable as believed—A comparison study of tree height estimates from field measurement, airborne laser scanning and terrestrial laser scanning in a boreal forest. *ISPRS Journal of Photogrammetry and Remote Sensing*, *147*, 132–145. <https://doi.org/10.1016/j.isprsjprs.2018.11.008>
- West, G. B., Enquist, B. J., & Brown, J. H. (2009). A general quantitative theory of forest structure and dynamics. *Proceedings of the National Academy of Sciences*, *106*(17), 7040–7045.
- Wright, I. J., Dong, N., Maire, V., Prentice, I. C., Westoby, M., Diaz, S., et al. (2017). Global climatic drivers of leaf size. *Science*, *357*(6354), 917–921. <https://doi.org/10.1126/science.aal4760>
- Wright, S. J., Jaramillo, M. A., Pavon, J., Condit, R., Hubbell, S. P., & Foster, R. B. (2005). Reproductive size thresholds in tropical trees: Variation among individuals, species and forests. *Journal of Tropical Ecology*, *21*(3), 307–315.
- Xu, K., Milliman, J. D., & Xu, H. (2010). Temporal trend of precipitation and runoff in major Chinese Rivers since 1951. *Global and Planetary Change*, *73*(3), 219–232. <https://doi.org/10.1016/j.gloplacha.2010.07.002>
- Zhao, X., Guo, Q., Su, Y., & Xue, B. (2016). Improved progressive TIN densification filtering algorithm for airborne LiDAR data in forested areas. *ISPRS Journal of Photogrammetry and Remote Sensing*, *117*, 79–91.
- Zhu, L., Yao, Q., Cooper, D. J., Han, S., & Wang, X. (2018). Response of *Pinus sylvestris* var. *mongolica* to water change and drought history reconstruction in the past 260 years, northeast China. *Climate of the Past*, *14*(8), 1213–1228.